

Firing Time Statistics for Driven Neuron Models: Analytic Expressions versus Numerics

Michael Schindler, Peter Talkner, and Peter Hänggi

Institut für Physik, Universität Augsburg, Universitätsstraße 1, D-86135 Augsburg, Germany

(Dated: October 30, 2018)

Analytical expressions are put forward to investigate the forced spiking activity of abstract neuron models such as the driven leaky integrate-and-fire model. The method is valid in a wide parameter regime beyond the restraining limits of weak driving (linear response) and/or weak noise. The novel approximation is based on a discrete state Markovian modeling of the full long-time dynamics with time-dependent rates. The scheme yields excellent agreement with numerical Langevin and Fokker-Planck simulations of the full non-stationary dynamics, not only for the first-passage time statistics, but also for the important interspike interval (residence time) distribution.

PACS numbers: 87.19.La, 05.40.-a, 87.18.Sn, 89.75.Hc

The detailed modeling of neural behavior presents a prominent challenge on the intriguing vista towards the understanding of neural coding principles. The leaky integrate-and-fire (LIF) model, whose deterministic formulation has been introduced long ago [1], likely is one of the most studied abstract neuron models [2]. It is characterized by marked simplicity and lack of memory: Whenever the neuron has been excited to fire a pulse it is reset to a predefined state. The beneficial rôle of an appreciable dose of noise has proved to bestow a key part to the interspike statistics of neurons [2]. There exist by now numerous studies and important generalizations of realistic synaptic models, mostly of a numerical nature, that demonstrate the rich behavior of the renewal firing probability, e.g. see in Ref. [3, 4, 5].

In presence of a time-dependent input-stimulation the stochastic firing process becomes non-stationary, which in turn significantly complicates the stochastic firing statistics. Nevertheless, the signal transmission and its detection can exhibit a remarkable improvement via the phenomenon of *Stochastic Resonance* [6]. The dynamics of the neuronal firing probability emerges due to a large bombardment of synaptic spike events; consequently, it is customary to employ a diffusion approximation for the stochastic dynamics of the membrane potential $x(t)$. The complexity of the driven abstract LIF model thus assumes the archetype, non-stationary Langevin dynamics

$$\dot{x}(t) = -\lambda x(t) + \mu + f(t) + \sqrt{2D}\xi(t) \quad (1)$$

where the process starts at a time s at $x(s) = x_0$ and fires when it reaches the threshold voltage $x = a$. Here, $f(t)$ presents a general, time-dependent stimulus which, for example, can be chosen to be oscillatory, and $\xi(t)$ is white Gaussian noise. The dynamics of the process $x(t)$ is equivalently described by a Fokker-Planck (FP) equation for the conditional probability density $\rho(x, t | x_0, s)$ in a time-dependent quadratic potential, $U(x, t) = \lambda[x - x_{\min}(t)]^2/2$ with $x_{\min}(t) = (\mu + f(t))/\lambda$,

reading

$$\partial_t \rho = L(t)\rho = \partial_x (U'(x, t)\rho) + D\partial_x^2 \rho, \quad (2)$$

with the absorbing boundary and initial conditions

$$\rho(a, t | x_0, s) = 0 \quad \text{for all } t, s, \text{ and } x_0 \quad (3)$$

$$\rho(x, s | x_0, s) = \delta(x - x_0). \quad (4)$$

After firing the process immediately restarts at the instantaneous minimum of the potential.

The set of eqs. (1–4) defines our starting point for obtaining the firing statistics of this driven neuron model. This is a rather intricate problem because the presence of non-stationarity and multiple time-scales for driving and relaxation, in combination with the absorbing boundary condition prohibits an analytical exact solution [7]. Our main objective is, nevertheless, to develop a most accurate analytical approximation that supersedes all prior attempts known to us. Those attempts, in fact, all involve the use of either of the following limiting approximation schemes such as the limit of linear response theory (i.e. a weak stimulus $f(t)$) [8], the limit of asymptotically weak noise [6, 9] or the use of the method of images which appears to present an uncontrollable approximation for the case with $\lambda \neq 0$ [4, 5]. A most appealing numerical approach is based on an exact integral equation for the first-passage time density of time-dependent Gauss-Markov processes with an absorbing boundary [10]. Our scheme detailed below yields novel analytic and tractable expressions beyond the linear response and weak noise limit; these are limited solely by the use of a discrete, Markovian stochastic dynamics for the population of the attracting domain and slowly varying (in comparison to intra-well relaxation time-scale) stimuli $f(t)$. As demonstrated below, this novel scheme indeed provides analytical formulae that compare very favorably with precise numerical results of the full dynamics in eqs. (1, 2–4). Different from other approaches, we obtain the distribution not only of the first-passage time but also of the residence time, which is the more interesting variable, concerning neurons.

To start, we approximate the solution to eqs. (2–4) in the regime where the statistics of times at which the threshold is reached can be characterized by a time-dependent firing rate $\kappa(t)$ [7, 11].

This rate then follows from a time-scale separation in the full FP dynamics (2) with boundary condition (3). After a few times λ^{-1} of the fast relaxation the probability density $\rho(x, t)$ assumes a slowly varying pattern that decays with the rate $\kappa(t)$. As in the time-independent case, this slowly varying part of $\rho(x, t)$ can be expressed by a product of the (normalized) instantaneous stationary solution $\rho_0(x, t) \propto \exp\{-U(x, t)/D\}$ to the FP equation, satisfying $L(t)\rho_0(x, t) = 0$, and a form function $\zeta(x, t)$. Our ansatz thus reads

$$\rho(x, t | x_0, s) \stackrel{(t-s) \gg \lambda^{-1}}{\simeq} \zeta(x, t) \rho_0(x, t) \exp\left(-\int_s^t \kappa(s') ds'\right). \quad (5)$$

The initial time s enters only through the exponential factor. The dependence of the conditional probability on the initial value x_0 decays exponentially on the timescale λ^{-1} and therefore can be neglected for long times.

Deep inside the attracting well, i.e. for $x \ll a$ there is no sensible difference between $\rho(x, t)$ and $\rho_0(x, t)$, and consequently $\zeta(x, t)$ approaches one. At the absorbing boundary, however, $\rho(a, t)$ and consequently $\zeta(a, t)$ both must vanish. The quantitative form of $\zeta(x, t)$ in the crossover region follows from

$$L^+(t)\zeta(x, t) = 0, \quad (6)$$

where the potential in the backward operator $L^+(t) = -U'(x, t)\partial_x + D\partial_x^2$ can be linearized about the threshold $x = a$. Eq. (6) then yields for the form function the result

$$\zeta(x, t) = 1 - \exp\left\{(x - a) \frac{U'(a, t)}{D}\right\}. \quad (7)$$

The rate $\kappa(t)$ is determined by multiplying the FP equation (2) in the long-time limit (5) by the form function $\zeta(x, t)$ and integrating over x from $-\infty$ to the threshold voltage a . In doing so, we account for prominent *finite barrier corrections*, yielding

$$\kappa(t) = -\frac{\int_{-\infty}^a dx \zeta(x, t) L(t) \zeta(x, t) \rho_0(x, t)}{\int_{-\infty}^a dx \zeta^2(x, t) \rho_0(x, t)}. \quad (8)$$

Upon insertion of eq. (7) for the form function one can exactly perform the integrations and obtains for the rate

$$\kappa(t) = \lambda \frac{\Delta U(t)}{D} \frac{1 - \operatorname{erf}(\sqrt{\Delta U(t)/D})}{1 - \exp(-\Delta U(t)/D)}, \quad (9)$$

where $\Delta U(t)$ denotes the instantaneous potential height at the threshold as seen from the minimum, and $\operatorname{erf}(z)$ is the error function. For very small D an expansion of the

error function leads to the well-known *weak noise* result for the time-dependent rate [6, 7], i.e.

$$\kappa^{\text{wn}}(t) = \lambda \sqrt{\Delta U(t)/(\pi D)} \exp(-\Delta U(t)/D). \quad (10)$$

Firing time distributions.—With the expression for the exit rate $\kappa(t)$ in (9) we can calculate the properties of interest, namely the densities for the first-passage time and the residence time [12] of the attracting ”integrating” state that covers the domain $-\infty < x(t) < a$.

The first-passage time distribution is given by the negative rate of change of probability finding the process at time t in the ”integrating” state, i.e.

$$g(t | s) = -\partial_t \int_{-\infty}^a \rho(x, t | x_0, s) dx \quad (11)$$

$$= \kappa(t) \exp\left(-\int_s^t \kappa(s') ds'\right), \quad (12)$$

Here, the integral over the spatial part of $\rho(x, t)$ yields unity and the exponential factor in (5) is obtained. It gives the probability for the process to stay in the ”integrating” state from time s until t without interruption.

The distribution of the residence times $h(\tau)$, also termed the *interspike interval density*, follows as the average of the first-passage time density over the density of resetting times s , which coincides with the firing rate $\kappa(s)$. It thus reads:

$$h(\tau) = \lim_{T \rightarrow \infty} \frac{\int_{-T}^T g(\tau + s | s) \kappa(s) ds}{\int_{-T}^T \kappa(s) ds}. \quad (13)$$

Equations (12) and (13), together with the expression for the rate (9) constitute the main results of this work. Their quantitative validity for an extended parameter regime will be checked next.

Numerical comparison.—We have employed three methods for the numerical analysis. A first one is based on the Langevin equation (1) where the position $x(t)$ is updated sequentially. For the second we have solved the FP equation (2) numerically, using a Chebychev collocation method to reduce the problem to a coupled system of ordinary differential equations, see also [13]. The third method solves an integral equation for the first-passage time probability density and is described in [10]. All three methods have provided practically identical results.

In the prior stimulating work [4] it has been left open in what relevant parameter regime the employed approximation possesses validity [5]. Here, using a periodic modulation $f(t) = A \cos(\omega t)$ we like to determine a minimal set of relevant parameters that can be taken for comparison with physiological measurements. The most general Langevin equation (1) considered has seven constant parameters, including the threshold a and the reset-position x_0 . Three of them, (λ, μ, a) , can be chosen to be $(1, 0, 1)$ by transforming to dimensionless coordinates,

using the time-unit λ^{-1} , the space-unit $(a - \mu/\lambda)$, and the coordinate-origin at μ/λ . The resulting parameters thus read (the bars indicate dimensionless coordinates)

$$\bar{A} = A/(\lambda a - \mu), \quad \bar{\omega} = \omega/\lambda, \quad \bar{D} = D/(\lambda(a - \mu\lambda)^2). \quad (14)$$

For our purposes it is advantageous to use instead the equivalent set

$$\bar{U}_+/\bar{D}, \quad \bar{U}_-/\bar{D}, \quad \text{and} \quad \bar{\omega}, \quad (15)$$

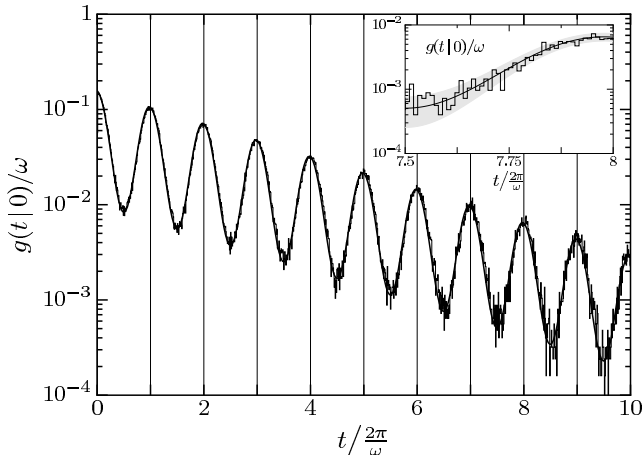


FIG. 1: First-passage time density for parameters $U_+/D = 8$, $U_-/D = 5$, $\omega = 0.05$. The jagged line depicts the histogram obtained from iterations of the Langevin equation in (16). Note that fluctuations in the histogram depend on the total number of events and the width of the histogram bins. These fluctuations stay completely within their expected range which is indicated as the gray shaded area in the inset. The height of this area is twice the expected standard deviation of the histogram levels. The solid line shows the analytic first-passage time density from eq. (12), with the rate used in (9). Both lines are in excellent agreement.

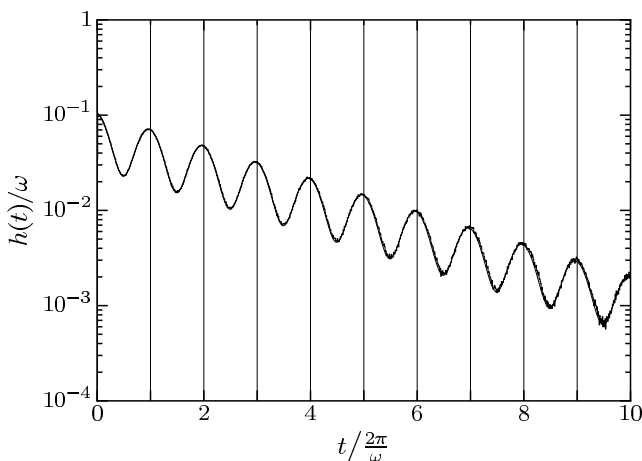


FIG. 2: Residence time density *vs.* time for the same parameters as in Fig. 1. The jagged line shows the histogram obtained from iterations of (16). Again, the numerics practically coincides within the line-width with the analytic expression in (13) evaluated with the rate in (9) (solid line).

where \bar{U}_+ and \bar{U}_- are the maximum and the minimum of $\bar{U}(1, \bar{t})$ during a whole period of modulation. These so chosen parameters have the benefit that they provide an on-hand estimate for the validity of our approximations and can be evaluated directly from (1).

The equation we have used in our simulations thus reads (omitting the overbars)

$$\dot{x}(t) = -x(t) + A \cos(\omega t) + \sqrt{2\bar{D}} \xi(t) \quad (16)$$

with the threshold located at $x = 1$. For obtaining the residence time, x has been reset into the minimum of $U(x, t)$ immediately after firing. The Figs. 1 and 2 depict the probability densities of the first-passage and the resi-

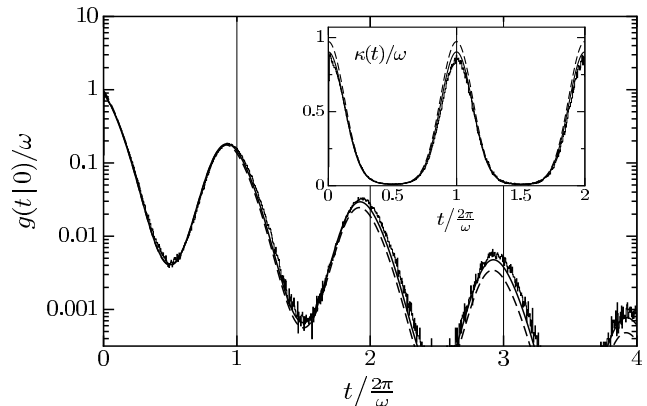


FIG. 3: Testing extreme limits. First-passage time density for an extremely small lower barrier $U_-/D = 3$. The remaining parameters are as in Fig. 1. Langevin simulation results (jagged), analytical result in (12) with eq. (9) (solid), likewise, with eq. (10) (dashed). The inset compares the rate $\kappa(t)$ obtained from simulations of (16) with the analytic results from eq. (9) and eq. (10), respectively.

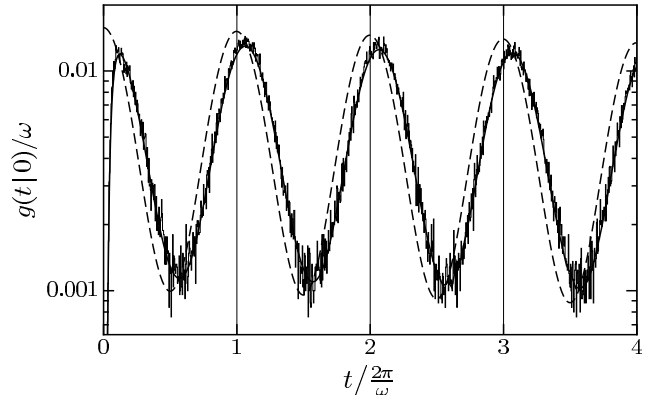


FIG. 4: Testing extreme limits. Probability density of the first-passage time for a very fast driving, $\omega = 0.5$. The other parameters are as in Fig. 1. The analytic approximation (eqs. (12) and (9), dashed line) still depicts maxima that are approximately located at $1, 2, \dots$ while the numerical results are shifted to later times. The jagged line presents the Langevin-iterations from (16). The solid curve presents within its linewidth both the numerical solution to the FP equation (2) and to the integral equation from [10].

dence times, respectively. The residence time distribution exhibits a less pronounced modulation in comparison with the first-passage time distribution. Both analytical expressions in (12) and (13) compare very favorably with the numerical results obtained by iteration of the Langevin equation (16). The remaining deviations in the two figures are of purely statistical nature (see the inset in Fig. 1) and can be diminished further by increasing the number of events in the simulations.

In order to further test the range of validity of our novel approximation scheme we – on purpose – have chosen extreme values for the lower barrier height U_-/D and angular driving frequency ω , respectively, see Figs. 3 and 4. Here, deviations from the numerical results are not the result of statistics but are systematic. For the low potential barrier in Fig. 3, the time-scales in the process are not separated sufficiently. The fast intra-well fluctuations begin to influence the behavior of the modulated firing dynamics. Moreover, the difference between the moderate noise result for the time-dependent rate $\kappa(t)$ in (9) and its weak noise approximation in (10) becomes visibly increased, as expected. Figure 4 depicts the other extreme situation with a modulation time-scale that is not slow enough. Because the system cannot follow the driving instantaneously we find a shift in the maxima of the first-passage time density. This shift is not reproduced by our approximation in (5) and (12); nevertheless, our scheme yields amazingly good results even within this extreme parameter regime. The results based on the numerical evaluation of the FP equation (2) and the integral equation [10] virtually collapse into one curve and perfectly coincide with the Langevin simulations. The same result was obtained for the other parameter values.

Conclusions.—The precise theoretical modeling of the neuronal spiking activity under external time-dependent driving presents a challenge of considerable importance in neurophysiology and physics. Due to the presence of non-stationarity, absorbing boundary conditions of the underlying first-passage problem and differing time-scales the task of obtaining reliable analytical estimates for the firing statistics is anything but trivial. By reference to a *discrete* Markovian dynamics for the corresponding full space-continuous stochastic dynamics we succeeded in obtaining analytical approximations for the time-dependent first-passage time and the residence time statistics that are valid beyond the restraining limits of linear response and asymptotically weak noise. We have tested our findings for the case of a periodically driven LIF model. The obtained agreement with precise numerical simulations of either the Langevin type in (16) or, equivalently, of the FP type in (2) turns out to be very good. Our method is not restricted to an oscillatory forcing but applies as well to arbitrary drive functions $f(t)$ such as an exponentially decaying drive (e.g. simulating a decaying threshold). Our scheme even yields good results in extreme parameter regimes where agreement

cannot be expected *a priori*.

Our method, primarily aimed at describing first-passage time and residence time probabilities of driven dynamical systems, is also readily extended to more realistic neuron models such as e.g. the two-dimensional driven FitzHugh-Nagumo model [14] for neuronal spiking activity, whose multiple attractors may be considered as discrete states. Likewise, the scheme can also be employed to study yet other time-dependent switching dynamics and synchronization phenomena such as the paradigm of *Stochastic Resonance* [6] and discrete or continuous Brownian motor transport [15].

This work has been supported by the Deutsche Forschungsgemeinschaft via Projects No. HA1517/13-4 and SFB-486, Projects No. A10 and No. B13.

-
- [1] L. Lapicque, J. Physiol. (Paris) **9**, 620 (1907).
 - [2] H. C. Tuckwell, *Stochastic Processes in the Neurosciences*, (SIAM, Philadelphia, 1989).
 - [3] B. W. Knight, J. Gen. Phys. **59**, 734 (1972); M. Stemmler, Network-Comp. Neural **7**, 687 (1996); P. Lansky, Phys. Rev. E **55**, 2040 (1997); M. T. Giraudo and L. Sacerdote, BioSystems **48**, 77 (1998); T. Shimokawa *et al.*, Phys. Rev. E **59**, 3461 (1999); H. E. Plesser and T. Geisel, Phys. Rev. E **59**, 7008 (1999); M. J. Chacron *et al.*, Phys. Rev. Lett. **85** 1576 (2000); N. Brunel *et al.*, Phys. Rev. Lett. **86**, 2186 (2001); L. Sacerdote and P. Lansky, BioSystems **67**, 213 (2002); J. W. Middleton *et al.*, Phys. Rev. E **68**, 021920 (2003); B. Lindner, A. Longtin and A. Bulsara, Neural Comp. **15**, 1761 (2003).
 - [4] A. R. Bulsara, T. C. Elston, C. R. Doering, S. B. Lowen, and K. Lindenberg, Phys. Rev. E **53**, 3958 (1996).
 - [5] H. E. Plesser and W. Gerstner, Neurocomputing **32–33**, 219 (2000); H. E. Plesser and T. Geisel, Phys. Rev. E **59**, 7008 (1999).
 - [6] L. Gammaitoni, P. Hänggi, P. Jung, and F. Marchesoni, Rev. Mod. Phys. **70**, 223 (1998).
 - [7] P. Hänggi, P. Talkner, and M. Borkovec, Rev. Mod. Phys. **62**, 251 (1990).
 - [8] B. Lindner and L. Schimansky-Geier, Phys. Rev. Lett. **86**, 2934 (2001); N. Fourcaud and N. Brunel, Neural Comp. **14**, 2057 (2002); B. Lindner *et al.*, Phys. Rep. **392**, 321 (2004).
 - [9] P. Jung and P. Hänggi, Phys. Rev. A **44**, 8032 (1991); V. A. Shneidman *et al.*, Phys. Rev. Lett. **72**, 2682 (1994); N. G. Stocks, Nuovo Cimento D **17**, 925 (1995); J. Lehmann, P. Reimann, and P. Hänggi, Phys. Rev. Lett. **84**, 1639 (2000); A. Nikitin, N. G. Stocks and A. R. Bulsara, Phys. Rev. E **68**, 016103 (2003); J. Casado-Pascual *et al.*, Phys. Rev. Lett. **91**, 210601 (2003).
 - [10] E. Di Nardo, A.G. Nobile, E. Pirozzi, L. M. Ricciardi, Adv. Appl. Probab. **33**, 453 (2001); A. Buonocore, *et al.*, Adv. Appl. Probab. **19**, 784 (1987).
 - [11] P. Talkner and J. Luczka, arXiv:condmat/0307498.
 - [12] R. Löfstedt and S. N. Coppersmith, Phys. Rev. E **49**, 4821 (1994); M. H. Choi, R. F. Fox, and P. Jung, Phys. Rev. E **57**, 6335 (1998); P. Talkner, Physica A **325**, 124 (2003).

- [13] J. Lehmann, P. Reimann, and P. Hänggi, Phys. Rev. E **62**, 6282 (2000).
- [14] R. A. FitzHugh, Biophys. J. **1**, 445 (1961); J. Nagumo, *et al.*, Proc. IRE **50**, 2061 (1962).
- [15] R. D. Astumian and P. Hänggi, Phys. Today **55** No.11, 33 (2002); P. Reimann, Phys. Rep. **361**, 57 (2002).